THE JOURNAL OF PHYSICAL CHEMISTRY C

Article

pubs.acs.org/JPCC

Glass-Forming Carbazolyl and Phenothiazinyl Tetra Substituted Pyrene Derivatives: Photophysical, Electrochemical, and Photoelectrical Properties

Renji R. Reghu,[†] Juozas V. Grazulevicius,*[,†] Jurate Simokaitiene,[†] Arunas Miasojedovas,[‡] Karolis Kazlauskas,[‡] Saulius Jursenas,[‡] Przemyslaw Data,[§,∥] Krzysztof Karon,[§,∥] Mieczyslaw Lapkowski,[§,∥] Valentas Gaidelis,[⊥] and Vygintas Jankauskas[⊥]

[†]Department of Organic Technology, Kaunas University of Technology, Radvilenu pl. 19, LT-50254 Kaunas, Lithuania

[‡]Institute of Applied Research, Vilnius University, Sauletekio 9-III, LT-10222 Vilnius, Lithuania

[§]Faculty of Chemistry, Silesian University of Technology, 44-100 Gliwice, Poland

[∥]Center of Polymer and Carbon Materials, Polish Academy of Science, 41-819 Zabrze, Poland

[⊥]Department of Solid State Electronics, Vilnius University, Sauletekio al. 9, LT-10222 Vilnius, Lithuania

ABSTRACT: Carbazolyl and phenothiazinyl tetra substituted derivatives of pyrene, namely, 1,3,6,8-tetra(9-ethyl-9*H*-carbazol-3-yl) pyrene (**1**), 1,3,6,8-tetra(9-ethyl-9*H*-carbazol-2-yl) pyrene (**2**), 1,3,6,8-tetra(10-ethyl-10*H*-phenothiazin-3-yl) pyrene (**3**) and 1,3,6,8-tetra(9-dodecyl-9*H*-carbazol-3-yl) pyrene (**4**), were synthesized and characterized. They displayed excellent thermal stability, with the onsets of thermal degradation well exceeding 400 °C, and demonstrated glass transitions between 32 and 232 °C. Pyrene derivatives with carbazole arms were shown to be highly fluorescent in dilute solution (fluorescence quantum yields, Φ_F, up to 0.84) and in rigid polymer matrix (Φ_F up to 0.60). They displayed significant emission quenching and shortening of the fluorescence decay time in neat films. In contrast, the phenothiazinyl-substituted pyrene derivative showed moderate fluorescence quantum efficiency in dilute solution (Φ_F = 0.21) or in polymer matrix (Φ_F = 0.25) and expressed intramolecular charge transfer character, which was revealed by the studies in different polarity media. The carbazolyl-substituted pyrene derivatives exhibited dicationic behavior and subsequently underwent electropolymerization as characterized by cyclic voltametry. Ionization potentials of thin layers of these materials measured by photoelectron spectroscopy ranged from 5.2 to 5.5 eV. Compound **4** showed hole-drift mobility of 5.8×10^{-5} cm^2 V^{-1} s^{-1} at an electric field of 10^6 V cm^{-1} as characterized by xerographic time-of-flight technique.

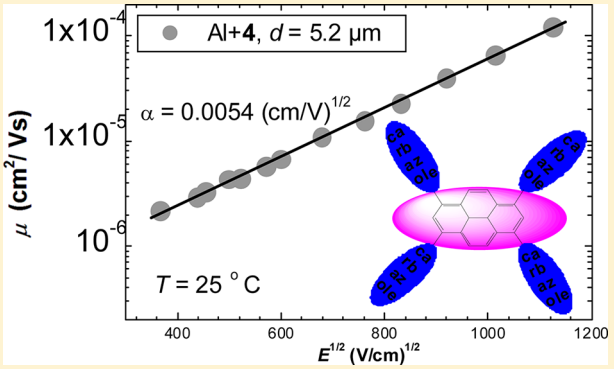

INTRODUCTION

Research from both academia and industry has been increasing consistently in the area of organic electronics during the past decades because of the great hunt for cost-effective devices such as organic light-emitting diodes, field-effect transistors, photovoltaic cells, sensors, etc.[1−4] Low-molar-mass organic electroactive materials possessing high fluorescence quantum yields and good charge transport properties are particularly interesting for application in organic light-emitting diodes.[5,6]

Conjugated molecules like star-shaped compounds or dendrimers with well-defined structure are of high scientific interest since their molecular size reaches the nanometer domain which brings them unique chemical and physical properties important for device applications.[7] The physical properties of such symmetric compounds can be tuned either by changing the core or by changing the arms. Accordingly various functional chromophores with different core−arm combinations have been reported.[8−11] Palladium catalyzed cross-coupling reactions like Suzuki reaction, Heck reaction, Stille cross coupling, or Sonogashira coupling have successfully been proven as convenient synthetic approaches for the preparation of such compounds.[11−14]

Organic materials consisting of the well-known polycyclic planar aromatic system, pyrene as a core, functionalized with different electron-donating chromophores as arms were employed as hole-transporting materials in various optoelectronic and electronic devices.[15,16] Additionally, such kind of architecture could facilitate the hole-injection by tuning the highest occupied molecular orbital (HOMO) energy level. On the other hand, the carbazole molecular moiety has been well

Received: February 29, 2012
Revised: June 28, 2012
Published: July 8, 2012

exploited for the preparation of both low-molar-mass and polymeric organic electroactive materials since they possess good chemical, environmental and electrochemical stability and the versatility in functionalization.[17−19] Moreover, it is interesting to note that the linking topology of the carbazole moiety has significant influence on the tunability of the physical properties of their derivatives.[20−22] The electron-rich phenothiazine is also extensively exploited in organic electronics because of the unique electro-optical properties of its derivatives and the resulting potential in diverse applications like organic electroluminescence or electrogenerated chemiluminescence.[23,24] Keeping these facts in mind we designed and synthesized pyrene-core based derivatives with the arms of differently linked carbazole and phenothiazine moieties. Properties of these derivatives were examined by performing thermal, optical, photophysical, electrochemical, and photoelectrical measurements.

EXPERIMENTAL SECTION

Materials. The starting compounds, i.e., 1,3,6,8-tetrabromopyrene, carbazole, and phenothiazine, were purchased from Sigma Aldrich and used as received. The reagents and the required materials, i.e., bromine, iodoethane, 1-bromododecane, *n*-butyl lithium, potassium hydroxide, sodium sulfate, potassium carbonate, 2-isopropoxy-4,4,5,5-tetramethyl-1,3,2-dioxaborolane, bis(triphenylphosphine) palladium(II) dichloride, and tetrabutylammonium tetrafluoroborate (Bu_4NBF_4), were also purchased from Sigma Aldrich and used as received. Silica gel (Sigma Aldrich) was used for column chromatography.

General Procedure for Suzuki−Miyaura Reactions. 1,3,6,8-Tetrabromopyrene (200 mg, 0.39 mmol) and the respective mono boronic acid pinacol esters (4.2 molar equiv) were dissolved in a solvent mixture of 20 mL of THF and 2 mL of water. Powdered potassium carbonate (6.6 molar equiv) was added and the reaction mixture was purged with nitrogen for 5 min. The reaction vessel was degassed and then, again purged with nitrogen. Bis(triphenylphosphine) palladium(II) dichloride (0.06 molar equiv) was added, and the mixture was stirred for 8−12 h at 80 °C under nitrogen. The reaction mixture was diluted with water and extracted using ethyl acetate. The organic layer was dried over sodium sulfate and evaporated. The crude product was purified by column chromatography using silica gel as the stationary phase. The solvent mixture of hexane and ethyl acetate in a volume ratio of 7:3 for **1**; 1:1 for **2**, and 9:1 for **4** and chloroform for **3** were used as eluents.

*1,3,6,8-Tetra(9-ethyl-9H-carbazol-3-yl) Pyrene (**1**).* Yield = 54%; yellow powder. ^{1}H NMR (300 MHz, $CDCl_3$, δ ppm): 8.50 (s, 4H), 8.36 (s, 4H), 8.33 (s, 2H), 8.19 (d, J = 2.3 Hz, 4H), 7.91 (dd, J = 3.4 Hz, 4H), 7.63 (d, J = 2.8 Hz, 4H), 7.55−7.48 (m, 8H), 7.27−7.24 (m, 4H), 4.49 (q, J = 7.1 Hz, 8H, NCH_2), 1.55 (t, J = 4.7 Hz, 12H, CH_3). IR (KBr, υ cm^{-1}): (arene C−H) 3047; (aliphatic C−H) 2974, 2930, 2890; (Ar C═C) 1625, 1600; (Ar C−N) 1471, 1459. Anal. Calc. for $C_{72}H_{54}N_4$: C, 88.67; H, 5.58; N, 5.74%. Found: C, 88.64; H, 5.79; N, 5.49%. MS (MALDI-TOF) m/z = 974.48 (exact mass = 974.43).

*1,3,6,8-Tetra(9-ethyl-9H-carbazol-2-yl) Pyrene (**2**).* Yield = 32%; yellow crystals. M.p.: 351−352 °C. ^{1}H NMR (300 MHz, $CDCl_3$, δ ppm): 8.39 (s, 4H), 8.35 (s, 2H), 8.31(d, J = 2.7 Hz, 4H), 8.23 (d, J = 2.5 Hz, 4H), 7.79(s, 4H), 7.67 (dd, J = 3.2 Hz, 4H), 7.57−7.47 (m, 8H), 7.33−7.28 (m, 4H), 4.50 (q, J = 7.1 Hz, 8H, NCH_2), 1.49 (t, J = 4.8 Hz, 12H, CH_3). IR (KBr, υ cm^{-1}): (arene C−H) 3048; (aliphatic C−H) 2970, 2929, 2890; (Ar C═C) 1626, 1599; (Ar C−N) 1471, 1456. Anal. Calc. for $C_{72}H_{54}N_4$: C, 88.67; H, 5.58; N, 5.74%. Found: C, 88.73; H, 5.39; N, 5.42%. MS (MALDI-TOF) m/z = 974.51 (exact mass = 974.43).

*1,3,6,8-Tetra(10-ethyl-10H-phenothiazin-3-yl) Pyrene (**3**).* Yield = 61%; dark yellow crystals. M.p.: 293−294 °C. ^{1}H NMR (300 MHz, $CDCl_3$, δ ppm): 8.19 (s, 4H), 7.93 (s, 2H), 7.48−7.44 (m, 8H), 7.23−7.18 (m, 8H), 7.06 (d, J = 2.9 Hz, 4H), 6.98−6.94 (m, 8H), 4.06 (q, J = 7 Hz, 8H, NCH_2), 1.53 (t, J = 4.7 Hz, 12H, CH_3). IR (KBr, υ cm^{-1}): (arene C−H) 3054; (aliphatic C−H) 2970, 2929, 2848; (Ar C═C) 1599, 1575; (Ar C−N) 1488, 1462. Anal. Calc. for $C_{72}H_{54}N_4S_4$: C, 78.37; H, 4.93; N, 5.08; S, 11.62%. Found: C, 78.75; H, 5.12; N, 4.84%. MS (MALDI-TOF) m/z = 1102.53 (exact mass = 1102.32).

*1,3,6,8-Tetra(9-dodecyl-9H-carbazol-3-yl) Pyrene (**4**).* Yield = 70%; pale yellow gummy solid. ^{1}H NMR (300 MHz, $CDCl_3$, δ ppm): 8.49 (s, 4H), 8.37 (s, 4H), 8.33 (s, 2H), 8.18 (d, J = 2.6 Hz, 4H), 7.91 (dd, J = 3.4 Hz, 4H), 7.62 (d, J = 2.8 Hz, 4H), 7.55−7.45 (m, 8H), 7.29−7.24 (m, 4H), 4.44−4.31(m, 8H, NCH_2), 2.03−1.88 (m, 8H, CH_2), 1.47−1.28 (m, 72H, CH_2), 0.89 (t, J = 4.2 Hz, 12H, CH_3). ^{13}C NMR (75.5 MHz, $CDCl_3$, δ ppm): 141.2, 140.0, 138.2, 132.3, 131.0, 128.9, 128.6, 126.7, 126.0, 125.8, 125.7, 123.3, 123.2, 122.7, 120.8, 119.1, 109.1, 108.7, 43.6, 32.2, 30.6, 29.9, 29.8, 29.7, 29.6, 29.3, 27.7, 25.1, 22.9, 14.4. IR (KBr, υ cm^{-1}): (arene C−H) 3048; (aliphatic C−H) 2922, 2851; (Ar C═C) 1626, 1599; (Ar C−N) 1489, 1465. Anal. Calc. for $C_{112}H_{134}N_4$: C, 87.56; H, 8.79; N, 3.65%. Found: C, 87.30; H, 9.03; N, 3.62%. MS (MALDI-TOF) m/z = 1534.91(exact mass = 1535.06).

Instrumentation. Nuclear magnetic resonance spectra were obtained using deuterated chloroform as a solvent with a Varian Unity Inova spectrometer operating at 300 and 75.5 MHz for ^{1}H and ^{13}C nuclei respectively. All of the data are given as chemical shifts δ (ppm) downfield from TMS. IR-spectroscopy measurements were performed on a Perkin-Elmer Spectrum GX spectrophotometer, using KBr pellets. The molecular weights of the target molecules were determined by MALDI-TOF using Shimadzu Biotech Axima Performance system and 2,5-dihydroxybenzoic acid (DHB) as the matrix under reflector mode of operation.

Differential scanning calorimetry measurements were performed on a Perkin-Elmer Pyris Diamond DSC apparatus at a heating/cooling rate of 10 °C min^{-1} under nitrogen atmosphere. Thermogravimetric analysis was executed on TA Instruments Q100 under nitrogen atmosphere at a heating rate of 20 °C min^{-1}.

Absorption spectra of the dilute solutions were recorded by a UV−vis−NIR spectrometer Lambda 950 (Perkin-Elmer). Photoluminescence (PL) of the derivative solutions and thin films was excited by a 365 nm wavelength light emitting diode (Nichia NSHU590-B) and measured using a back-thinned CCD spectrometer (Hamamatsu PMA-11). For these measurements dilute solutions of the investigated compounds were prepared by dissolving them in spectral grade tetrahydrofuran (THF) at 1 × 10^{-5} M concentration. Neat films of the investigated compounds were prepared from the 1 × 10^{-3} M THF solutions on the quartz substrates by drop-casting technique. The same technique was also employed to form solid solutions (0.25 wt %) in polystyrene (PS). Fluorescence quantum yield (Φ_F) of the samples was estimated by utilizing an integrating sphere (Sphere Optics) coupled to the CCD

dx.doi.org/10.1021/jp3019952 | J. Phys. Chem. C 2012, 116, 15878−15887

spectrometer using optical fiber. Fluorescence transients were measured using a time-correlated single photon counting system Pico Harp 300 (Pico Quant GmbH). Pulsed excitation at 1 MHz repetition rate was provided by a picosecond diode laser with a pulse duration of 70 ps and an emission wavelength of 375 nm.

Electrochemical investigations were carried out using AUTOLAB potentiostat "PGSTAT20". The data were collected using GPES (General Purpose Electrochemical System) software. The electrochemical cell was comprised of a platinum wire with 1 mm diameter of working area as the working electrode, Ag/AgCl electrode as the reference electrode, and platinum coil as the auxiliary electrode. Cyclic voltamperometric measurements were conducted at room temperature, and for all measurements, the Ag/AgCl reference electrode was calibrated against ferrocene/ferrocenium redox couple. The experiments were carried out in 0.1 M solution of Bu_4NBF_4 in dichloromethane (anhydrous HPLC grade). The concentrations of solutions of **1**, **2**, and **4** were 1 mM and of **3** was 0.3 mM. UV−vis−near IR spectroelectrochemical analysis was performed on an HP Agilent 8453 spectrometer. The spectroelectrochemical cell consisted of indium tin oxide (ITO) covered glass with 1 cm^2 working area as the working electrode, Ag wire as the quasi-reference electrode, and platinum coil as the auxiliary electrode. Electron spin resonance (ESR) spectroelectrochemical analysis was performed on JEOL JES-FA200, and the spectroelectrochemical cell was comprised of platinum wire as the working electrode, Ag wire as the quasi-reference electrode, and platinum coil as the auxiliary electrode.

The ionization potentials (I_p) were measured by photoelectron spectroscopy in air as described earlier.[25] The materials were dissolved in chloroform and coated onto Al plates precoated with ∼0.5 μm thick methylmethacrylate and methacrylic acid copolymer (MKM) adhesive layer. The function of MKM layer is not only to improve adhesion but also to eliminate the electron photoemission from the Al layer. In addition, this layer is conductive enough to avoid charge accumulation on it during the measurements. The thickness of the layers was ca. 0.5 μm.

The hole-drift mobility of compound **4** was estimated by the xerographic time-of-flight method.[26,27] The sample for the measurement was prepared by drop casting of the solution of compound **4** in tetrahydrofuran onto a polyester film with an Al layer. After coating the sample was heated at 70 °C for 1 h. Thus the transporting layer of the sample was prepared. The thickness of the transporting layer was ∼5 μm. Hole drift-mobility (μ) was measured in the xerographic mode. The electric field was created by positive corona charging. The charge carriers were generated at the layer surface by illumination with pulses of nitrogen laser (pulse duration was 1 ns, wavelength 337 nm). As a result of pulse illumination the layer surface potential decreases up to 2−5% of the initial potential. The capacitance probe connected to the wide frequency band electrometer measured the speed of the surface potential decrease dU/dt. The transit time t_t for the samples with the transporting material was determined by the kink on the curve of the dU/dt transient in log−log scale. The drift mobility was calculated by using the formula $\mu = d^2/U_0 t_t$, where d is the layer thickness and U_0 is the surface potential at the moment of illumination.

RESULTS AND DISCUSSION

Synthesis. The chemical structures of the synthesized compounds are shown in Figure 1. The target materials, i.e., **1**−**4**, were synthesized from 1,3,6,8-tetrabromopyrene by Suzuki−-Miyaura coupling reactions as described in Scheme 1.

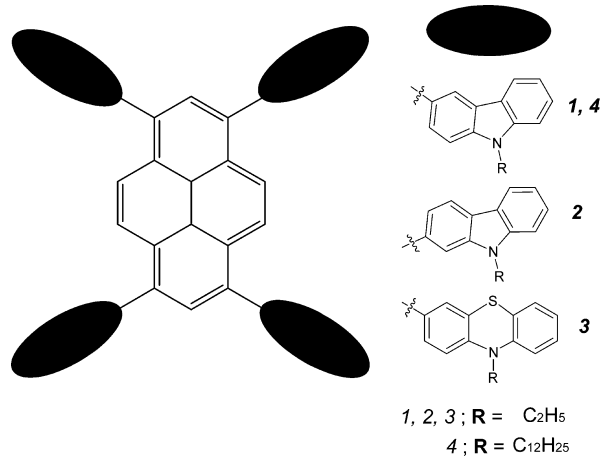

Figure 1. Chemical structures of compounds **1**−**4**.

The respective key intermediates for the preparation of **1** and **4**, i.e., 9-ethyl-9*H*-carbazol-3-yl boronic acid pinacol ester (**3-eCZ**) and 9-dodecyl-9*H*-carbazol-3-yl boronic acid pinacol ester (**3-dCZ**), were synthesized from 3-bromo carbazole by N-alkylation and subsequent borylation using 2-isopropoxy-4,4,5,5-tetramethyl-1,3,2-dioxaborolane as reported elsewhere.[28,29] 9-Ethyl-9*H*-carbazol-2-yl boronic acid pinacol ester (**2-eCZ**) was synthesized by the nitration of 4-bromo biphenyl followed by its ring closure with triphenylphosphine and the consequent N-alkylation and borylation as reported in the literature.[30−32] The intermediate compound for the synthesis of **3**, 10-ethyl-10*H*-phenothyazen-3-yl boronic acid pinacol ester (**3-ePZ**), was synthesized by the established literature procedure starting from phenothiazine.[33,34] The synthesized compounds were purified by column chromatography and characterized by NMR and IR spectroscopy, MALDI-TOF and elemental analysis. The spectral and elemental analysis data are in good agreement with their chemical structures.

Thermal Properties. The behavior under heating of compounds **1**−**4** was studied by differential scanning calorimetry (DSC) and thermogravimetric analysis (TGA) under a nitrogen atmosphere. The values of glass transition temperatures (T_g) and the temperatures of the onsets of the thermal decomposition (T_{ID}) are collected in Table 1. Compounds **2**−**3** were isolated after the synthesis and purification as crystalline materials. However they could be transformed into the glassy state by cooling from the melt. Compounds **1**−**3** showed endothermic melting transitions during the first DSC heating scans (Table 1). However they exhibited clear glass transitions when the cooled isotropic melts were further heated (Figure 2). The DSC thermogram of compound **1** is shown in Figure 2a. For compound **1**, the first heating scan showed a glass transition followed by a structural relaxation through crystallization at 345 °C and a melting transition at 431 °C. However, the cooling scan and the second heating scan only showed glass transitions and not any other kind of thermal transitions such as crystallization or melting, which clearly demonstrated the transformation of the crystalline

dx.doi.org/10.1021/jp3019952 | J. Phys. Chem. C 2012, 116, 15878−15887

Scheme 1. Synthetic Route for the Preparation of Compounds 1−4[a]

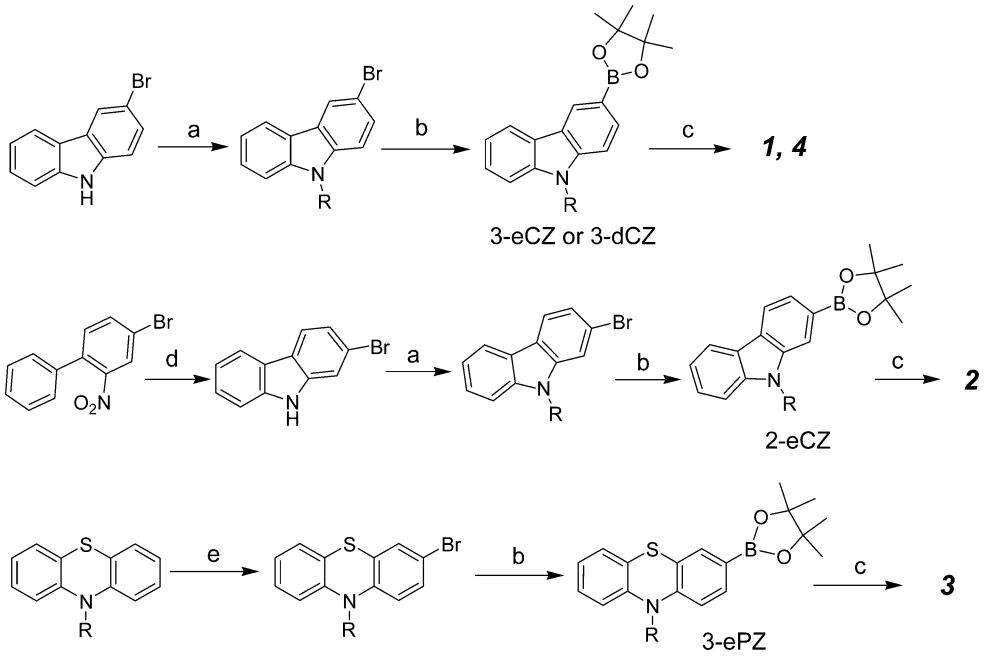

[a]Reagents and conditions: (a) C_2H_5I or $C_{12}H_{25}Br$, KOH, DMF, RT, 24 h; (b) *n*-BuLi, 2-isopropoxy-4,4,5,5-tetramethyl-1,3,2-dioxaborolane, THF, −78 °C to RT, 10−12 h; (c) 1,3,6,8-tetrabromopyrene, $Pd(Ph_3)_2Cl_2$, K_2CO_3, THF/H_2O, 80 °C, 8−12 h; (d) PPh_3, *ortho*-dichlorobenzene, 180 °C, 12 h; (e) Br_2, AcOH/NaOH, $CHCl_3$, 0 °C, 2 h.

Table 1. Thermal Characteristics of Compounds 1−4

compound	T_g[a] (°C)	T_m[b] (°C)	T_{ID}[c] (°C)
1	232	431	537
2	216	409	512
3	211	324	418
4	32		452

[a]Glass transition temperature. [b]Melting temperature. [c]Thermal decomposition onset.

phase into the amorphous (glassy) phase.[35] Compounds **1**−**3** showed very high T_g ranging from 211 to 232 °C. Compound **4** was isolated after the synthesis and purification as amorphous material and exhibited T_g just above the room temperature.

All of the synthesized pyrene derivatives (**1**−**4**) exhibited high thermal stability with the decomposition onset temperatures ranging from 418 to 537 °C. It was found that both the attached chromophores and the *N*-alkyl substituents affect the thermal stability of pyrene derivatives. The thermal stability of topological isomers **1** and **2** were comparable, whereas compound **4** with longer *N*-alkyl substituents displayed lower thermal degradation temperature. The phenothiazinyl derivative exhibited lower thermal decomposition temperature compared to the carbazolyl derivatives.

Optical and Photophysical Properties. Absorption and PL spectra of dilute solutions in THF, dilute solid solutions in PS, and neat films of the pyrene derivatives (**1**−**4**) are depicted in Figure 3. The details of the optical properties of the derivatives are summarized in Table 2. Compounds **1** and **4** differing only in the alkyl chain length of the carbazole moiety showed very similar spectral properties in the dilute solutions, PS matrixes and in the neat films. As expected, Φ_F of the two compounds in a diluted form (in solution or PS matrix) are also nearly the same, i.e., 0.83−0.84 in the solution and 0.58−0.60 in the polymer matrix. Interestingly, a difference in the alkyl

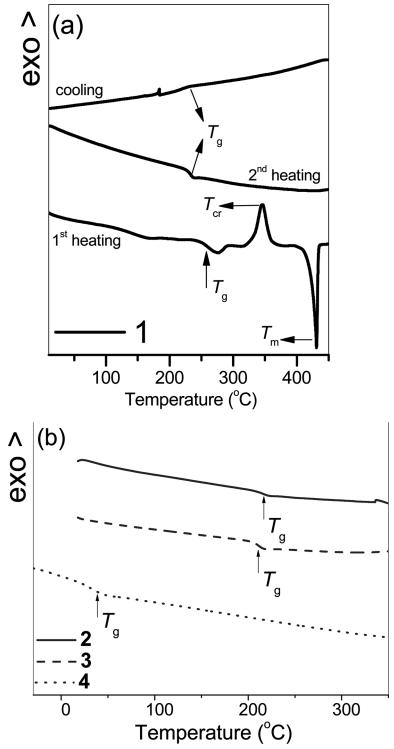

Figure 2. DSC thermograms of (a) **1** and (b) **2**, **3**, and **4** (during second heating scan). Heating/cooling rate: 10 °C min^{-1} under nitrogen atmosphere.

chain length of compounds **1** and **4** has almost no effect on the PL spectrum and PL quantum yield of the neat films, which most likely signifies similar amorphous packing of the films prepared by solution-casting technique. The lowest energy absorption band of the carbazolyl-substituted pyrene derivatives

dx.doi.org/10.1021/jp3019952 | J. Phys. Chem. C 2012, 116, 15878−15887

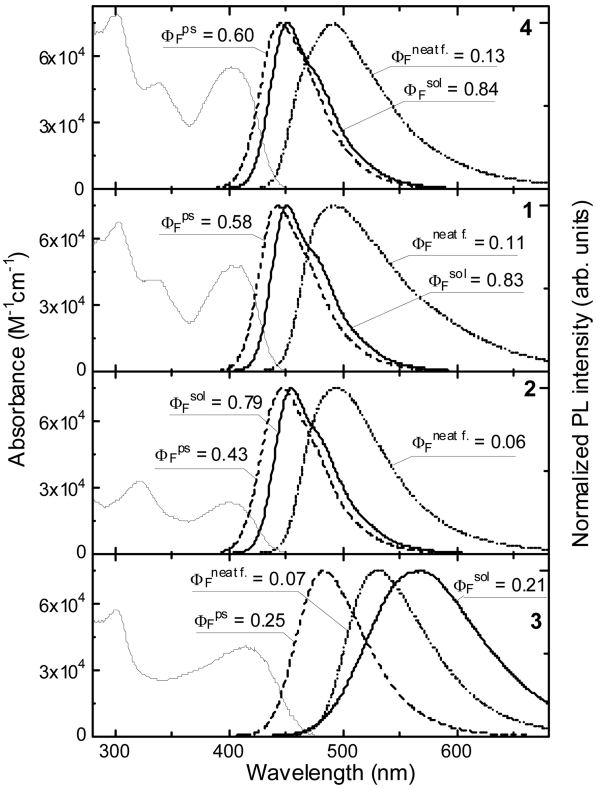

Figure 3. Absorption spectra of the pyrene derivatives **1**–**4** in dilute THF solutions (thin solid line) and normalized PL spectra of the derivatives **1**–**4** in dilute THF solutions (thick solid line), dilute solid solutions in PS (0.25 wt %; thick dashed line), and neat films (thick dotted line). Estimated fluorescence quantum yields (Φ_F) indicated.

1, **2**, and **4** is located at ca. 400 nm irrespectively of the linking (2- or 3-position) topology of the carbazolyl moiety, followed by the alike Stokes shifts in THF solution. Note somewhat weaker absorbance of the band at 403 nm for the solution of derivative **2** as compared with that for the solutions of derivatives **1** and **4**. This correlates with slightly decreased Φ_F (0.79) of the compound **2** solution. Taking into account that the onset of absorption of individual pyrene and carbazole moieties is below 350 nm with PL emerging at 355–375 nm,[36–38] the considerably red-shifted spectra of the studied pyrene derivatives clearly point out extension of the pyrene-core conjugation to the carbazole arms. This observation is in agreement with a strong enhancement of the $S_0 \rightarrow S_1$ transition of pyrene substituted at 1, 3, 6, or 8 positions; however, unsubstituted or 2- and 7-substituted pyrene has vanishingly small oscillator strength.[39] A more detailed analysis of the lowest energy absorption and fluorescence band shapes of the pyrene derivatives **1**, **2**, and **4** in dilute solutions reveals that they are not mirror images of each other. Particularly, the absorption bands are broad and unstructured, whereas several vibronic modes can be resolved in PL spectra. The presence of the vibronic replicas in the PL indicates enhanced molecule rigidity in the excited state as compared to that in the ground state. It is likely that in the ground state the singly bridged carbazole substituents are twisted with respect to the pyrene core due to the steric hindrance. Highly nonplanar geometry of the molecule facilitates intramolecular torsional motions, which smear out the vibronic structure of the absorption band. As opposed to this, in the excited state the twist angle between carbazole moieties and the pyrene core reduces so that the molecule becomes more planar and thus expresses enhanced conjugation and rigidity. To verify the planarization of the pyrene derivatives upon excitation, the derivatives were introduced into rigid polymer matrixes at low concentration (0.25 wt %) where molecule twisting in the excited state was suppressed.[40] Unable to planarize the derivatives exhibited reduced Φ_F as well as slightly blue-shifted PL spectra due to reduced conjugation in the PS matrix as compared to those in solution (Figure 3). This result in turn confirms a tendency of the singly bonded carbazole-substituted pyrene derivatives **1**, **2** and **4** to planarize in the excited state resulting in the increased conjugation and emission efficiency.

PL spectra of the neat films of the pyrene derivatives **1**, **2**, and **4** are broadened and shifted to the long wavelengths by ca. 40 nm as compared to those of dilute solutions or solid solutions in PS. This observation can be attributed to the intermolecular interaction in the neat films. The bathochromic shift accompanied by the 6–13-fold reduction in Φ_F of the neat films with respect to that of the solutions can result from intermolecular coupling of exciton transition dipole moments promoting excitation migration via a hopping process to nonradiative decay centers (distortions, defects, etc.).

Interestingly, pyrene derivative **3** with more polar phenothiazine arms (with respect to carbazole arms) exhibits different spectral behavior. The absorption and PL spectra of dilute solutions of **3** are much broadened, unstructured, and significantly red-shifted with respect of those of carbazole-substituted pyrene derivatives **1**, **2**, and **4**. The large Stokes shift (of 150 nm) of the PL band can arise from photoinduced intramolecular charge transfer (ICT), which is solvent polarity dependent.[41] The presence of ICT character in the derivative **3** was confirmed by spectral measurements using the solvents of different polarity, such as hexane, chloroform, and THF. Indeed, the measurements revealed strong bathochromic shift of the PL maximum from 470 nm for the solution in nonpolar hexane to 570 nm for the solution in polar THF while maintaining almost unchanged Φ_F. Since the fluorescence quantum efficiencies of the pyrene derivative **3** in the dilute solution (nonviscous medium) and in the PS matrix (highly

Table 2. Absorption and Fluorescence Data of Dilute (10^{-5} M) THF Solutions, Solid 0.25 wt % Solutions in PS, and Neat Films of Carbazolyl (1, 2, and 4) and Phenothiazinyl (3) Substituted Pyrene Derivatives

	solution				neat film			PS film		
	λ_{abs} [a], nm	λ_{em} [b], nm	Φ_F [c]	τ [d], ns	λ_{em}, nm	Φ_F	τ_{avg}, ns	λ_{em}, nm	Φ_F	τ, ns
1	403	451	0.83	1.6	493	0.11	1.7	443	0.58	1.8
2	400	455	0.79	1.5	496	0.06	1.3	446	0.43	1.5
3	415	567	0.21	2.1	533	0.07	0.9	483	0.25	1.6
4	403	451	0.84	1.7	491	0.13	1.8	445	0.60	1.9

[a] λ_{abs}, absorption maxima. [b] λ_{em}, emission maxima. [c] Φ_F, fluorescent quantum yield. [d] τ, fluorescent decay time constant.

dx.doi.org/10.1021/jp3019952 | J. Phys. Chem. C 2012, 116, 15878–15887

viscous medium) are also similar 0.21−0.25, molecular planarization in the excited state is unlikely. Thus, dramatic PL spectral shifts observed for derivative **3** observed in different media, i.e., solution, polymer matrix, and neat film, are a consequence of ICT character of the derivative and result from the changes in polarity of the surroundings.

To study excited state relaxation dynamics in carbazolyl- and phenothiazinyl-substituted pyrene derivatives, PL transients were measured (Figure 4). The dilute solutions of carbazolyl-

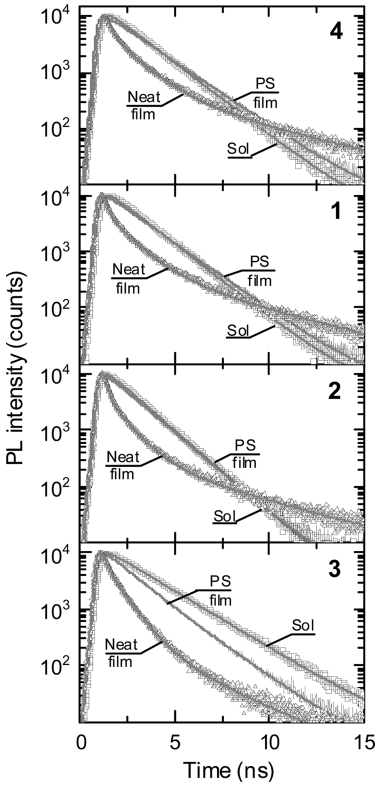

Figure 4. PL transients of dilute THF solutions, neat films, and PS films (doped at 0.25 wt %) of the carbazolyl- (**1**, **2**, and **4**) and phenothiazinyl-substituted (**3**) pyrene derivatives. Lines are single or multiexponential fits of the data.

substituted derivatives **1**, **2**, and **4** exhibited single exponential decay with decay time constants (τ) of 1.5−1.7 ns, whereas dilute solution of phenothiazinyl-substituted compound **3** showed slightly longer τ of 2.1 ns. PL decays of all of the pyrene derivatives molecularly dispersed in the PS matrix at 0.25 wt % were found to be similar to those of their dilute THF solutions, whereas PL transients of the neat films expressed clearly nonexponential behavior. The nonexponential transients with rapid excited state relaxation in an early stage (ca. 1−3 ns after excitation pulse) and prolonged relaxation at a later stage (ca. 5 ns after excitation) are typically observed in a solid state, where exciton migration and localization at lower energy states take place (spectral diffusion).[40] During the initial exciton migration stage, migration-induced exciton quenching at nonradiative decay centers occurs, which drastically degrades Φ_F of the neat films of the pyrene derivatives (Figure 3). Localized at lower energy states excitons evade fast nonradiative decay and, therefore, exhibit prolonged relaxation times.

Electrochemical Properties. The electrochemical behavior of compounds **1**−**4** in dichloromethane (DCM) was examined by cyclic voltametry (CV). It was found that the carbazolyl substituted compounds undergo multielectron oxidation processes and the redox potentials were dependent on the molecular structure. A reversible redox process was observed for all of the derivatives at low oxidation potential region (up to first oxidation peak) and a quasi-reversible characteristic was noted for the second oxidation peak. Figure 5 illustrates oxidation processes of pyrene derivatives in 0.1 M Bu_4NBF_4/DCM solutions. The electrochemical investigation of 1 mM solution of pyrene in 0.1 M Bu_4NBF_4/DCM solution revealed the oxidation potential at 0.54 V versus Ag/AgCl calibrated against Fc/Fc^+ redox couple which suggested that the first oxidation potential of investigated compounds might be from pyrene core.[42,43] For compounds **1**, **2**, and **4**, the second oxidation peak was in the range of 0.81 to 1 V versus Ag/AgCl and was comparable with that of the previously reported carbazole derivatives.[44,45] Hence, the second oxidation process of these compounds can apparently be due to the presence of electron donor-substituents, i.e., carbazoles. Phenothiazinyl-substituted derivative **3** seems to be less stable in the electrochemical environment compared to the carbazolyl-substituted derivatives and assumed to be degraded during successive scanning.

Figure 5 shows pronounced increases in anodic current intensity for tetra carbazolyl substituted pyrene derivatives, **1**, **2**, and **4**, during the successive voltametric scanning. This observation suggests the occurrence of electro-polymerization on the working electrode. A slight potential shift was observed in the oxidation redox process of compound **4** during the course of electro-polymerization which suggested the hindrance of the doping BF_4^- anions from doping−dedoping processes due to the presence of long dodecyl chains. The phenothiazinyl derivative **3** was not electro-polymerized on the anode. This might be either due to the low solubility of **3** in dichloromethane since the electro-polymerization reactions are dependent on monomer concentration or due to the presence of less reactive phenothiazinyl tetra substituents. For electro-polymerization to be initiated minimum concentration of radical ions should be generated in the reaction medium which might be restricted, in the case compound **3**, due to the decreased availability of electroactive species in less concentrated electrolyte.

Figure 6 demonstrates the cyclic voltammograms of electrochemically generated polymers of **1**, **2**, and **4** (i.e., **P1**, **P2**, and **P4**, respectively) in monomer-free electrolyte. The redox potentials, HOMO−LUMO energy levels, and electrochemical bandgaps of **P1**, **P2**, and **P4** are collected in Table 3. These values are calculated from the first oxidation and reduction potential onsets according to the established equations:[46]

$$I_p = -(E_p + 4.8) \quad [\text{eV}]$$

$$E_A = -(E_n + 4.8) \quad [\text{eV}]$$

where the ionization potential (I_p) is related to the HOMO and the electron affinity (E_A) is related to the LUMO. E_n and E_p are the onset reduction and oxidation potentials versus Fc/Fc^+.

As it can be seen from the CV profiles, carbazolyl-containing polymers are highly conductive and electrochemically stable. Electrochemically synthesized polymers **P1**, **P2**, and **P4** containing carbazole moieties were assumed to possess network-like structures. Furthermore, the electro-polymerization might occur at the sixth position of carbazole moieties irrespective of the nature of monomers **1**, **2**, and **4** in which

dx.doi.org/10.1021/jp3019952 | J. Phys. Chem. C 2012, 116, 15878−15887

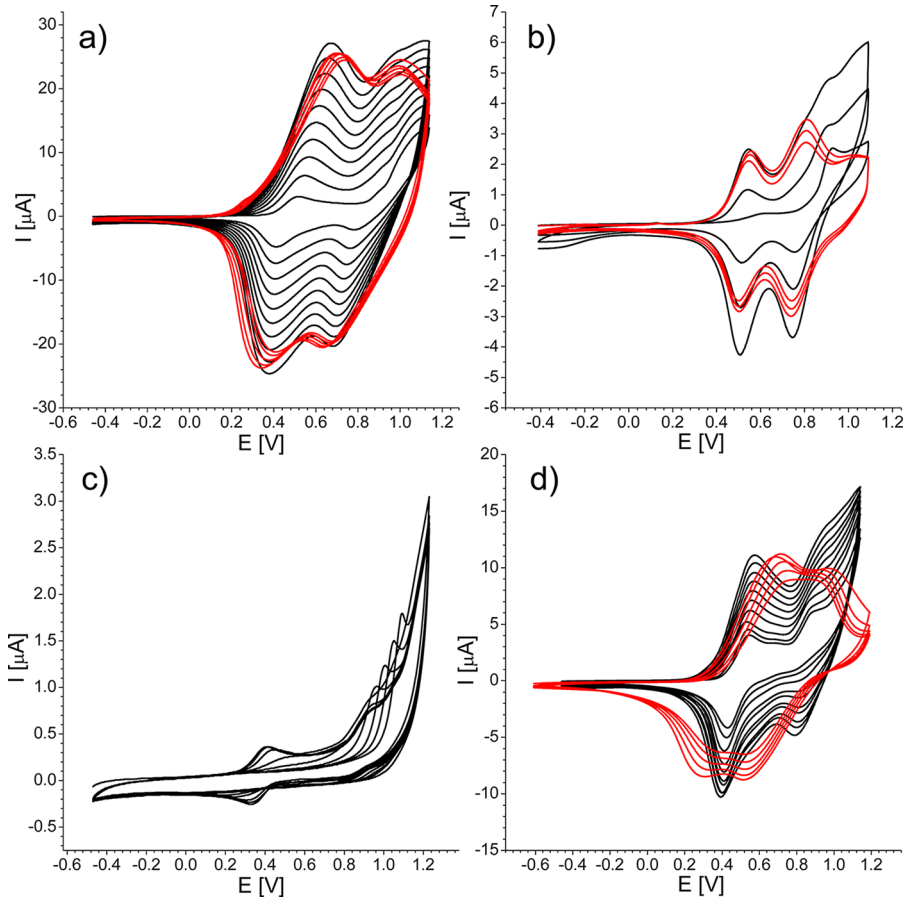

Figure 5. Cyclic voltammograms of pyrene derivatives (black lines) showing repetitive anodic sweeps at a platinum electrode immersed in a solution of compounds **1** (a), **2** (b), **3** (c), and **4** (d). Red lines demonstrate the doping−dedoping process of their electrodeposited films in monomer free medium. Measurement conditions: scan rate 50 mV/s, Ag/AgCl reference electrode, 0.1 M Bu_4NBF_4/dichloromethane electrolyte.

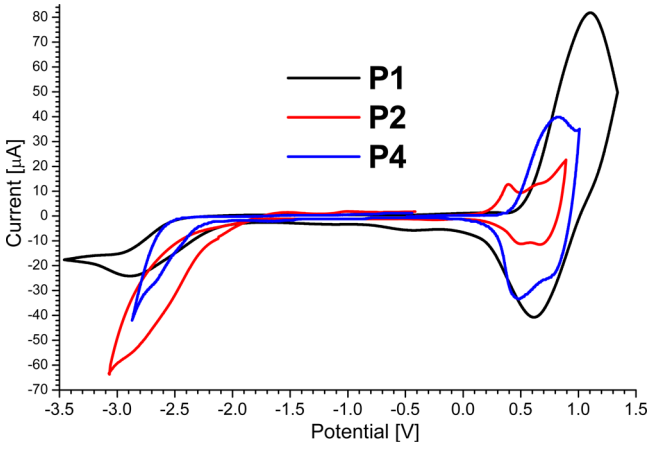

Figure 6. Cyclic voltammograms of electrodeposited polymers **P1**, **P2**, and **P4** at the platinum electrode in monomer free medium. Measurement conditions: scan rate 300 mV/s, Ag/AgCl reference electrode, 0.1 M Bu_4NBF_4/dichloromethane electrolyte.

carbazolyl groups are linked differently to the pyrene core. It is known that the third and sixth positions of carbazole derivatives are more electron rich and, hence, more reactive toward electro-polymerization compared to the second and seventh positions.[44] Polymer **P2** possessed the lowest oxidation potential as compared to those of the other derivatives which might be due to the slight increase in effective conjugation length due to the presence of 2-substituted carbazolyl segments in the polymer backbone.[47] It is interesting to note that **P1** possessed the low-lying HOMO and LUMO levels compared to those of **P2**. Moreover, the electrochemically determined band gap was rather high for **P1** compared to that of **P2**. This observation can be explained by the greater distortion in 3-substituted carbazolyl derivative due to the benzidine-like linkage to pyrene core compared to 2-substituted carbazolyl derivative possessing terphenyl-like linkage which in turn, influences the effective conjugation length of the respective polymers.[47−49] Comparatively similar electrochemical band gaps of polymers **P1** and **P4** suggested that the electro-polymerization might occur through the same position (i.e., sixth position) of carbazole moieties albeit they differ slightly in the HOMO−LUMO levels.

Spectroelectrochemical properties of the electro-deposited films of the selected carbazolyl-containing polymers, **P1** and **P2**, on ITO coated glass electrode were investigated by UV−vis−near IR analysis. The absorption spectra of polymers **P1** and **P2** recorded as a function of increasing applied electrode potentials are shown in Figure 7. It is found that the absorption band corresponding to the electro-deposited polymers, for example; λ_{max} = 302 nm for **P1** and λ_{max} = 311 nm for **P2**, gradually decreases with the increase of the applied voltage. Moreover for polymers **P1** and **P2**, new definite absorption bands also appeared at ca. 418, ca. 685, and beyond 900 nm during the doping processes. This observation might be explained by the formation of charged species such as polarons and bipolarons.[50]

dx.doi.org/10.1021/jp3019952 | J. Phys. Chem. C 2012, 116, 15878−15887

Table 3. Electrochemical Characteristics of Electro-Deposited Polymers P1, P2, and P4[a]

compound	E_{ox1}[b] (V)	E_{red}[c] (V)	E_{ox1}^{onset} (V)	E_{red}^{onset} (V)	HOMO (eV)	LUMO (eV)	E_g^{eld} (eV)
P1	1.1	0.61−2.78	0.53	−2.11	−5.33	−2.69	2.64
P2	0.39	0.47−2.29	0.3	−2.1	−5.1	−2.7	2.4
P4	0.82	0.45−2.67	0.42	−2.27	−5.22	−2.53	2.69

[a]Potentials vs Ag/AgCl calibrated against Fc/Fc^+. Working electrode Pt, 0.1 M Bu_4NPF_4−CH_2Cl_2, scan rate 300 mV/s. [b]E_{ox1}, first oxidation potential. [c]E_{red}, reduction potential. [d]E_g^{el}, electrochemical bandgap.

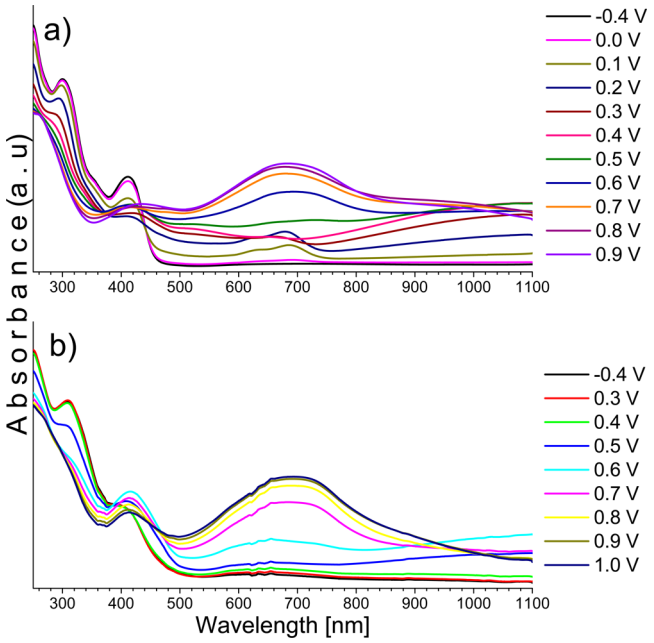

Figure 7. Absorption spectra of electro-deposited films of **P1** (a) and **P2** (b) on ITO electrode at various applied potentials in monomer free 0.1 M Bu_4NBF_4/dichloromethane electrolyte.

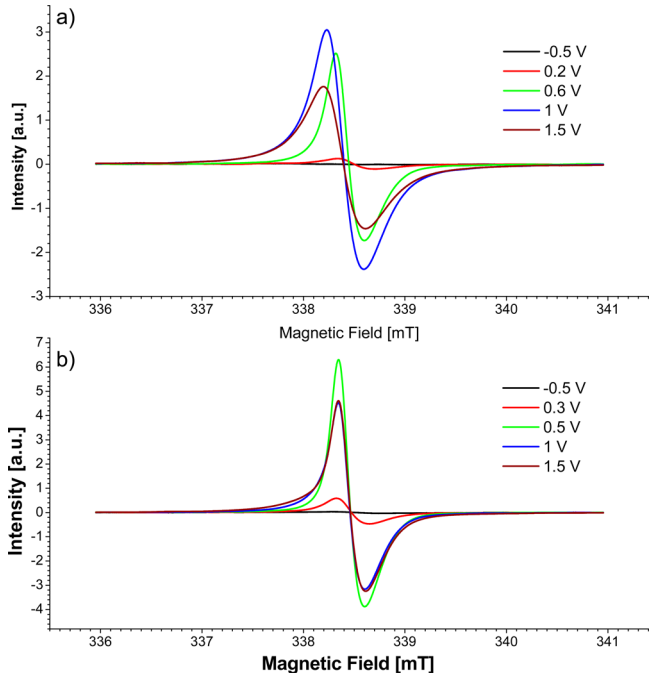

Figure 8. ESR spectra of electrochemically doped polymeric films **P1** (a) and **P2** (b) on platinum electrode at various applied potentials in monomer free 0.1 M Bu_4NBF_4/dichloromethane electrolyte.

The absorption peak located at ca. 685 nm is apparently due to the formation of bipolarons, whereas the spectral bands appeared in lower and higher energy regions might be due to the formation of polaronic species.[50,51] As a result of p-doping, the color of the electrodeposited films changed from light green to dark violet which implies that these polymeric films have the potential for application in electrochromic devices.[52]

The formation of polarons and bipolarons was confirmed by ESR spectroscopy. For recording of ESR spectra, polymers **P1** and **P2** were electro-deposited on a platinum electrode. ESR spectra of polymers **P1** and **P2** recorded during the doping processes are demonstrated in Figure 8. At low oxidation potentials the electro-deposited polymers showed symmetrical signals corroborating the formation of polarons.[53] On further doping, the increase in the spectral intensity can be attributed to the creation of more poloronic species. The deceased spectral intensity as well as increased spectral broadening at very high doping levels suggested the formation of low-spin bipolarons.[53,54]

Photoelectrical Properties. Ionization potentials (I_p) of thin solid layers of the synthesized compounds were measured by photoelectron spectroscopy. Photoelectron emission spectra of **1**−**4** are shown in Figure 9. The intersection points of the linear parts of the spectra drawn with the abscissa axis give the ionization potential values. I_p values of tetra substituted pyrene derivatives range from 5.2 to 5.5 eV. Compounds **1** and **4** exhibited similar I_p values as expected, whereas **2**, the

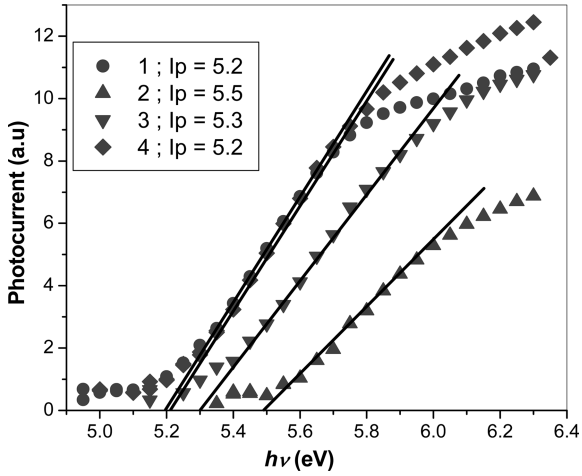

Figure 9. Photoelectron spectra and ionization potentials (in eV) of the thin films of compounds **1**−**4**.

regioisomer of **1**, demonstrated a higher I_p level compared to **1** and **4**.

Room temperature hole-drift mobility (μ_h) of a thin layer of **4** was measured by xerographic time-of-flight (XTOF) technique. The representative dU/dt transient for the neat film of **4** is demonstrated in Figure 10. It exhibits dispersive hole-transport. The hole-transit times (t_t) needed for the

dx.doi.org/10.1021/jp3019952 | J. Phys. Chem. C 2012, 116, 15878−15887

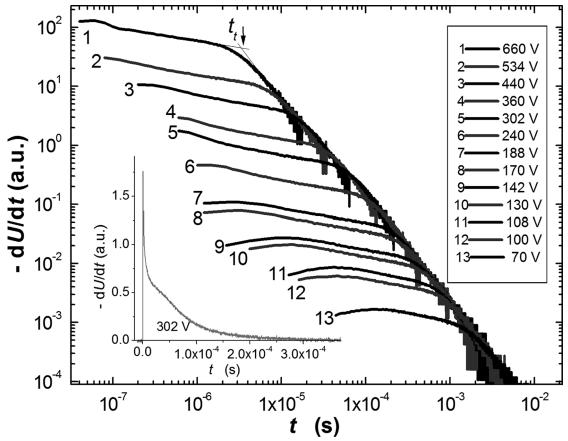

Figure 10. XTOF transients for the neat film of **4**. A 1 ns laser operating at 337 nm was used. T = 25 °C. The arrow mark indicate transit time of holes at respective surface voltage.

estimation of hole mobilities were established from intersection points of two asymptotes from the double-logarithmic plots. The electric field dependency of hole-drift mobility of the layer of **4** in air is shown in Figure 11. The linear dependency of

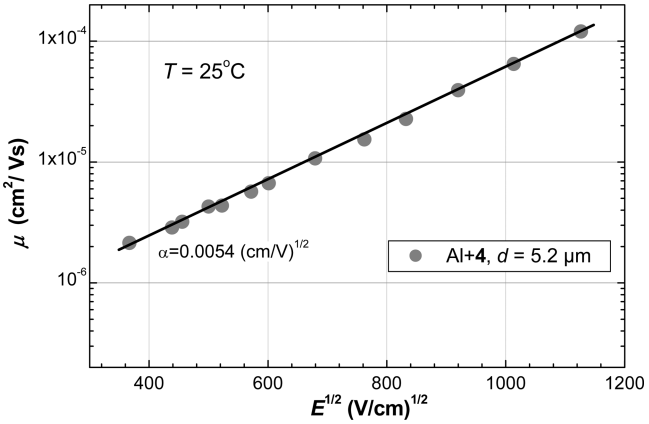

Figure 11. Electric field dependency of hole drift-mobility of the layer of **4**.

hole-drift mobility on the square root of electric field (E) is observed. The hole-drift mobility value of 5.8×10^{-5} cm^2 V^{-1} s^{-1} was observed for the thin solid layer of compound **4** at an electric field of 10^6 Vcm^{-1} at 293 K.

CONCLUSIONS

Carbazolyl and phenothiazinyl tetra substituted pyrene derivatives were synthesized and characterized, and their thermal, electrochemical, photophysical, and photoelectrical properties were studied. The synthesized compounds exhibit high thermal stability with the temperatures of the onsets of the thermal decomposition exceeding 400 °C. They form molecular glasses with high glass transition temperatures. Carbazole arms in the tetra functionalized pyrene derivatives are found to be twisted with respect to the pyrene core; however, the molecules tend to planarize in the excited state, thus increasing molecule conjugation and fluorescence quantum yields up to 0.84 in dilute solutions. The compounds also display high fluorescence quantum yields (up to 0.60) when molecularly dispersed in polymer films at low concentration. In the neat films they show fluorescence decay time shortening (in the initial stage) and considerable drop in fluorescence quantum efficiency, which indicates exciton-migration-induced quenching at nonradiative decay sites. Moderate fluorescence quantum efficiency (0.21) exhibiting phenothiazinyl-substituted pyrene derivative exhibits significant PL spectral shifts in different polarity media, which is attributed to intramolecular charge transfer. The redox-active carbazolyl-substituted pyrene derivatives exhibit dicationic behavior and subsequently undergo electro-polymerization. Ionization potentials of thin layers of these materials ranged from 5.2 to 5.5 eV. Carbazolyl-substituted pyrene derivative **4** transports holes with the drift mobility of 5.8×10^{-5} cm^{2}V^{-1}s^{-1} at an electric field of 10^6 V cm^{-1} as characterized by the XTOF technique.

AUTHOR INFORMATION

Corresponding Author

*Fax: +37037 300152. Tel: +37037 300193. E-mail: juozas.grazulevicius@ktu.lt.

Notes

The authors declare no competing financial interest.

ACKNOWLEDGMENTS

This research work was supported by FP-7 PEOPLE PROGRAMME, Marie Curie Actions−ITN Grant No. 215884. A. Swinarew (University of Silesia, Poland) is thanked for MALDI-TOF measurements. A. Sakalyte (University Rovira & Virgili, Spain) is thanked for the TGA measurements.

REFERENCES

(1) Sasabe, H.; Kido, J. *Chem. Mater.* **2011**, *23*, 62.
(2) Kim, H. N.; Guo, Z. Q.; Zhu, W. H.; Yoon, J.; Tian, H. *Chem. Soc. Rev.* **2011**, *40*, 79.
(3) Pron, A.; Reghu, R. R.; Rybakiewicz, R.; Cybulski, H.; Djurado, D.; Grazulevicius, J. V.; Zagorska, M.; Kulszewicz-Bajer, I.; Verilhac, J.-M. *J. Phys. Chem. C* **2011**, *115*, 15008.
(4) Walker, B.; Kim, C.; Nguyen, T.-Q. *Chem. Mater.* **2011**, *23*, 470.
(5) Oha, H.-Y.; Lee, C.; Lee, S. *Org. Electron.* **2009**, *10*, 163.
(6) Strohriegl, P.; Grazulevicius, J. V. *Adv. Mater.* **2002**, *14*, 1439.
(7) Han, Y.; Fei, Z.; Sun, M.; Bo, Z.; Liang, W. Z. *Macromol. Rapid Commun.* **2007**, *28*, 1017.
(8) Kanibolotsky, A. L.; Perepichka, I. F.; Skabara, P. J. *Chem. Soc. Rev.* **2010**, *39*, 2695.
(9) Metri, N.; Sallenave, X.; Beouch, L.; Plesse, C.; Goubard, F.; Chevrot, C. *Tetrahedron Lett.* **2010**, *51*, 6673.
(10) Huang, H.; Fu, Q.; Zhuang, S.; Mu, G.; Wang, L.; Chen, J.; Ma, D.; Yang, C. *Org. Electron.* **2011**, *12*, 1716.
(11) Jiang, Z.; Ye, T.; Yang, C.; Yang, D.; Zhu, M.; Zhong, C.; Qin, J.; Ma, D. *Chem. Mater.* **2011**, *23*, 771.
(12) Operamolla, A.; Farinola, G. M. *Eur. J. Org. Chem.* **2011**, 423.
(13) Mishra, A.; Ma, C.-Q.; Janssen, R. A. J.; Buerle, P. *Chem.—Eur. J.* **2009**, *15*, 13521.
(14) Krüger, H.; Janietz, S.; Sainova, D.; Dobreva, D.; Koch, N.; Vollmer, A. *Adv. Funct. Mater.* **2007**, *17*, 3715.
(15) Sonar, P.; Soh, M. S.; Cheng, Y. H.; Henssler, J. T.; Sellinger, A. *Org. Lett.* **2010**, *12*, 3293.
(16) Xing, Y.; Xu, X.; Zhang, P.; Tian, W.; Yu, G.; Lu, P.; Liu, Y.; Zhu, D. *Chem. Phys. Lett.* **2005**, *408*, 169.
(17) Lengvinaite, S.; Grazulevicius, J. V.; Grigalevicius, S.; Gub, R.; Dehaen, W.; Jankauskas, V.; Zhang, B.; Xie, Z. *Dyes Pigm.* **2010**, *85*, 183.
(18) Simokaitiene, J.; Grazulevicius, J. V.; Jankauskas, V.; Rutkaite, R.; Sidaravicius, J. *Dyes Pigm.* **2008**, *79*, 40.
(19) Figueira-Duarte, T. M.; Müllen, K. *Chem. Rev.* **2011**, *111*, 7260.
(20) Tomkeviciene, A.; Grazulevicius, J. V.; Jankauskas, V. *Chem. Lett.* **2008**, *37*, 344.

(21) Tomkeviciene, A.; Grazulevicius, J. V.; Kazlauskas, K.; Gruodis, A.; Jursenas, S.; Ke, T. H.; Wu, C. C. *J. Phys. Chem. C* **2011**, *115*, 4887.
(22) Reghu, R. R.; Bisoyi, H. K.; Grazulevicius, J. V.; Anjukandi, P.; Gaidelis, V.; Jankauskas, V. *J. Mater. Chem.* **2011**, *21*, 7811.
(23) Cao, H.; Chen, Z.; Liu, Y.; Qu, B.; Xu, S.; Cao, S.; Lan, Z.; Wang, Z.; Gong, Q. *Synth. Met.* **2007**, *157*, 427.
(24) Lai, R. Y.; Kong, X.; Jenekhe, S. A.; Bard., A. J. *J. Am. Chem. Soc.* **2003**, *125*, 12631.
(25) Ostrauskaite, J.; Voska, V.; Buika, G.; Gaidelis, V.; Jankauskas, V.; Janeczek, H.; Sidaravicius, J.; Grazulevicius, J. V. *Synth. Met.* **2003**, *18*, 4577.
(26) Montrimas, E.; Gaidelis, V.; Pazera, A. *Lithuanian J. Phys.* **1966**, *6*, 578.
(27) Vaezi-Nejad, S. M. *Int. J. Electronics* **1987**, *62*, 361.
(28) Li, Z.; Li, Z.; Di, C.; Zhu, Z.; Li, Q.; Zeng, Q.; Zhang, K.; Liu, Y.; Ye, C.; Qin, J. *Macromolecules* **2006**, *39*, 6951.
(29) Tavasli, M.; Bettington, S.; Bryce, M. R.; Batsanov, A. S.; Monkman, A. P. *Synthesis* **2005**, *10*, 1619.
(30) Freeman, A. W.; Urvoy, M.; Criswell, M. E. *J. Org. Chem.* **2005**, *70*, 5014.
(31) Percec, V.; Obata, M.; Rudick, J. G.; De, B. B.; Glodde, M.; Bera, T. K.; Magonov, S. N.; Balagurusamy, V. S. K.; Heiney, P. A. *J. Polym. Sci., Part A: Polym. Chem.* **2002**, *40*, 3509.
(32) Tang, W.; Lin, T.; Ke, L.; Chen, Z. *J. Polym. Sci., Part A: Polym. Chem.* **2008**, *46*, 7725.
(33) Ebdrup, S. *J. Chem. Soc., Perkin Trans.* **1998**, *1*, 1147.
(34) Krämer, C. S.; Zimmermann, T. J.; Sailer, M.; Müller, T. J. J. *Synthesis* **2002**, *9*, 1163.
(35) Shirota, Y. *J. Mater. Chem.* **2000**, *10*, 1.
(36) Simokaitiene, J.; Grigalevicius, S.; Grazulevicius, J. V.; Rutkaite, R.; Kazlauskas, K.; Jursenas, S.; Jankauskas, V.; Sidaravicius, J. *J. Optoelectron. Adv. Mater.* **2006**, *8*, 876.
(37) Basuray, G.; Chakraborty, I.; Moulik., S. *J. Colloid Interface Sci.* **2006**, *294*, 248.
(38) Romero-Ale, E. E.; Olives, A. I.; Martín, M. A.; del Castillo, B.; López-Alvarado, P.; Menéndez, J. C. *Luminescence* **2005**, *20*, 162.
(39) Crawford, A. G.; Dwyer, A. D.; Liu, Z.; Steffen, A.; Beeby, A.; Palsson, L.-O.; Tozer, D. J.; Marder, T. B. *J. Am. Chem. Soc.* **2011**, *133*, 13349.
(40) Karpicz, R.; Puzinas, S.; Krotkus, S.; Kazlauskas, K.; Jursenas, S.; Grazulevicius, J. V. *J. Chem. Phys.* **2011**, *134*, 204508.
(41) Acar, N.; Kurzawa, J.; Fritz, N.; Stockmann, A.; Roman, C.; Schneider, S.; Clark, T. *J. Phys. Chem. A* **2003**, *107*, 9530.
(42) Zhang, C.; Xu, Y.; Wang, N.; Xu, Y.; Xiang, W.; Ouyang, M.; Ma, C. *Electrochim. Acta* **2009**, *55*, 13.
(43) Xu, L.; Zhao, J.; Liu, R.; Liu, H.; Liu, J.; Wang, H. *Electrochim. Acta* **2010**, *55*, 8855.
(44) Ambrose, J. F.; Nelson, R. F. *J. Electrochem. Soc. Electrochem. Sci.* **1968**, 1159.
(45) Tidwell, C. P.; Alexander, L. A.; Fondren, L. D.; Belmore, K.; Nikles, D. E. *Indian J. Chem.* **2007**, *46*, 1658.
(46) Lapkowski, M.; Data, P.; Golba, S.; Soloducho, J.; Nowakowska-Oleksy, A. *Opt. Mater.* **2011**, *22*, 1445.
(47) Morin, J.-F.; Leclerc, M.; Ades, D.; Siove, A. *Macromol. Rapid Commun.* **2005**, *26*, 761.
(48) de Halleux, V.; Calbert, J.-P.; Brocorens, P.; Cornil, J.; Declercq, J-P.; Brédas, J.-L.; Geerts, Y. *Adv. Funct. Mater.* **2004**, *14*, 649.
(49) Sonntag, M.; Kreger, K.; Hanft, D.; Strohriegl, P. *Chem. Mater.* **2005**, *17*, 3031.
(50) Pomerantz, Z.; Zaban, A.; Ghosh, S.; Lellouche, J.-P.; Garcia-Belmonte, G.; Bisquert, J. *J. Electroanal. Chem.* **2008**, *614*, 49.
(51) van Haare, J. A. E. H.; Havinga, E. E.; van Dongen, J. L. J.; Janssen, R. A. J.; Cornil, J.; Bredas, J.-L. *Chem.—Eur. J.* **1998**, *4*, 1509.
(52) Otero, L.; Sereno, L.; Fungo, F.; Liao, Y.-L.; Lin, C.-Y.; Wong, K.-T. *Chem. Mater.* **2006**, *18*, 3495.
(53) Taerum, T.; Lukoyanova, O.; Wylie, R. G.; Perepichka, D. F. *Org. Lett.* **2009**, *11*, 3230.
(54) Domagala, W.; Pilawa, B.; Lapkowski, M. *Elecrochim. Acta* **2008**, *53*, 4580.